Geometries and energies of the excited states of pyridazine studied by sac and sac CI calculations

ARTICLE *in* CHEMICAL PHYSICS · AUGUST 1986

Impact Factor: 1.65 · DOI: 10.1016/0301-0104(86)85061-3

Chemical Physics 107 (1986) 81–87
North-Holland, Amsterdam

GEOMETRIES AND ENERGIES OF THE EXCITED STATES OF PYRIDAZINE STUDIED BY SAC AND SAC CI CALCULATIONS

Masahide TERAZIMA, Seigo YAMAUCHI, Noboru HIROTA

Department of Chemistry, Faculty of Science, Kyoto University, Kyoto 606, Japan

Osamu KITAO and Hiroshi NAKATSUJI

Division of Molecular Engineering, Graduate School of Engineering, Kyoto University, Kyoto 606, Japan

Received 16 October 1985; in final form 18 April 1986

The geometries and energies of the ground and excited states of pyridazine are calculated by an ab initio calculation which includes electron correlation. It is found that electron correlation plays an essential role in determining the geometries of the excited states. The optimized geometry of the T_1 state as well as that of the ground state are planar. On the other hand, the force constant along the twisted mode of the N–N bond in the T_1 state is much smaller than that in the ground state. It is suggested that this distorted potential produces a large Franck–Condon factor between the T_1 and S_0 states, which leads to a very large radiationless decay rate constant of the T_1 state. The location of the S_2 origin is discussed on the basis of the present results.

1. Introduction

Properties of the excited states of diazines have been subject of numerous experimental and theoretical studies. Pyridazine with two nitrogen atoms adjacent to each other has spectroscopic properties very different from those of other diazines, such as pyrazine and pyrimidine, but the detailed nature of the excited states has not been well understood. Here we first discuss some of the relevant properties of the excited states of pyridazine.

Phosphorescence of pyridazine has never been observed under any conditions, which makes a striking contrast to the strongly phosphorescent characters of pyrazine and pyrimidine. This non-phosphorescent character has attracted attention of many investigators and suggestions have been made concerning the possible reasons for the lack of phosphorescence [1–7]. For instance, inefficient S_1–T_1 intersystem crossing (ISC) was thought to be responsible for the non-phosphorescent character by several groups [1–3]. Another suggested possible mechanism involves rapid back ISC from T_1 to a forbidden S_1' state below the fluorescent S_1 state [8]. Recently, however, we have succeeded in detecting the EPR signal of the T_1 state of pyridazine by the time resolved EPR (TREPR) technique with laser excitations and demonstrated that the T_1 state possesses nearly pure $^3n\pi^*$ character with an unusually short lifetime of ≈ 1 μs in rigid glass at 3.0 K [9]. This experiment shows that the short lifetime is due to very rapid T_1–S_0 ISC, but neither to the T_1–S_1' ISC suggested by Cohen and Goodman [9] nor to photochemical processes.

The radiationless decay rate constant of $^3n\pi^*$ pyridazine is larger than those of $^3n\pi^*$ pyrazine and pyrimidine by a factor of 2×10^4 and it is desirable to understand the mechanism of such a fast decay. Since the T_1–S_0 radiationless decay strongly depends on the geometry of the T_1 state, reliable knowledge about the structure of the T_1 state is indispensable for understanding the mechanism. Unfortunately, our present knowledge

0301-0104/86/$03.50

about the geometries of the excited states of pyridazine is very meager. The geometry of the T_1 state was calculated by the PPP extended method [10] and the INDO method [11], but the results are mutually inconsistent. The N–N bond length in the T_1 state obtained by the PPP method is longer than that in the ground state, while the INDO calculation indicates a shorter bond length in the T_1 state.

An other question about the excited states is related to the location of the $S_2(B_1)$ state. Innes et al. [12] suggested that the band at 373 cm^{-1} above the S_1 origin in the absorption spectrum is the origin of the $S_2(B_1(n\pi^*))$ state. This assignment was also supported by the more recent spectroscopic work of Ueda et al. [13]. However, existence of such nearly degenerate low-lying excited states has never been justified by semi-empirical MO calculations [14] and the validity of such an assignment has not been established definitively.

In order to answer these unsolved questions we have attempted to obtain information about the geometries and the energies of the excited states of pyridazine from ab initio calculations including electron correlation. Geometry optimization was performed at the Hartree–Fock (HF) level of approximation, and at a more elaborate level of approximation which includes considerable amounts of electron correlation. For the latter, we used the symmetry-adapted-cluster (SAC) expansion for the ground state and the SAC CI theory for the excited states [15,16]. These methods are based on a cluster expansion of the wavefunction and are established as a reliable method for calculating geometries of ground and excited states [17]. They take account of the electron correlations in the ground and excited states in a well balanced way. These methods have been successfully applied to the valence and Rydberg excitations and ionizations of CO_2, NO_2 [16], ethylene [17], formaldehyde [18], NO radical [19], pyrrole, furan, and cyclopentadiene [20]. Here we discuss the geometries of the excited states and the mechanism for the very fast T_1–S_0 radiationless transition. The main conclusion is that electron correlation is important in determining geometries of the excited states.

2. Calculation

Geometry optimization was performed using the STO-3G minimal basis set with the GAMESS program [22]. The HF method is used for the ground state geometry and the open-shell restricted HF method is used for the $^3B_1$ and $^3A_2$ states. The optimized geometries were determined within the restriction of C_{2v} (planar) and C_2 (non-planar) symmetries.

The energies of the ground and excited states were calculated by the SAC and SAC CI methods, respectively [15,16]. The reference MOs were calculated with the GAMESS program by using the STO-3G and 4-31G double-zeta basis sets. We did not include a Rydberg-type basis set and the diffuse $d\pi$-type AOs which are important for the description of relatively higher excited states [17–20]. Though our basis sets are quite restricted, the calculation should provide reliable results for the geometries of the low-lying states, because diffuse AOs are not considered to be important in determining their geometry.

The set of active MOs consists of 15 occupied orbitals and all the virtual orbitals in the calculation at the STO-3G level. In the calculation at the 4-31G level, we used 12 occupied and 30 virtual orbitals for the active MOs. To reduce the size of calculations, we selected the linked operators as in ref. [15]. The thresholds λ_g and λ_e were 3.0×10^{-5} and 7.0×10^{-5}, respectively, and the dimensions of the matrices involved were about 2000 in the 4-31G case. In the STO-3G case, λ_g and λ_e were 1.0×10^{-4}, and the dimensions of the calculation were about 1000.

3. Results and discussion

3.1. The geometry of the ground state

The optimized geometry of the ground state (Q_0) at the HF level is shown in fig. 1. The geometry obtained with the restriction of C_{2v} symmetry is the same as that with C_2 symmetry. The calculated bond lengths and the bond angles are given in table 1 together with the experimental values. With this geometry, the SAC and SAC CI

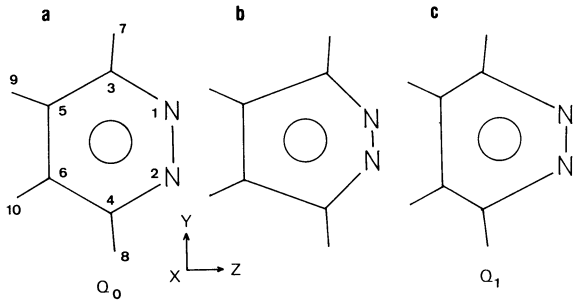

Fig. 1. The optimized geometries of (a) the ground state (Q_0), (b) the $^3A_2(n\pi^*)$ state and (c) the $^3B_1(n\pi^*)$ state at the HF level of approximation with the restriction of C_{2v} symmetry (Q_1). In the cases (b) and (c), the differences from Q_0 are exaggerated. Molecular axes and atomic number are also shown.

calculations were performed at the 4-31G level to obtain the wavefunctions and energies of the ground and excited states. The calculated energies are shown in table 2 with the experimental results.

3.2. The geometry of the $^3A_2(n\pi^*)$ state

The geometry obtained with the HF approximation is shown schematically in fig. 1. The bond distances and angles are listed in table 1. The optimized geometry with the C_2 symmetry is the same as that with the C_{2v} symmetry. The geometry is similar to that of the ground state except for the decreased N–N bond length. This decrease can be explained by excitation of an electron from

Table 1
The bond lengths and angles of pyridazine

	S_0 (calc)	S_0[a] (exp)	$^3A_2(n\pi^*)$	$^3B_1(n\pi^*)$ (C_{2v} sym.)
r_{12} (Å)	1.363	1.330	1.236	1.291
r_{13} (Å)	1.347	1.341	1.380	1.416
r_{35} (Å)	1.397	1.393	1.461	1.336
r_{56} (Å)	1.371	1.377	1.337	1.465
r_{37} (Å)	1.086	1.064	1.076	1.085
r_{59} (Å)	1.082	1.064	1.082	1.081
∠137 (deg)	115.1	111.7	119.0	116.1
∠359 (deg)	120.2	122.7	117.4	120.6

[a] Ref. [21].

Table 2
The vertical transition energies (cm^{-1}) of pyridazine for the geometry optimized in S_0

State	Energy (calc.)	Energy (obs.) [a]
$^3B_1(n\pi^*)$	28422	22487(0–0)
$^1B_1(n\pi^*)$	34540	26600(0–0)
$^3B_2(\pi\pi^*)$	35687	
$^3A_2(n\pi^*)$	37698	
$^1A_2(n\pi^*)$	41090	

[a] Ref. [12].

the n_- antibonding orbital to the π_2 orbital possessing a bonding character in the N–N bond region (fig. 2).

3.3. Geometry of the $^3B_1(n\pi^*)$ state

The optimized geometry of the $T_1(B_1(n\pi^*))$ state is somewhat complicated. At the HF level under the assumption of planar geometry (C_{2v} symmetry) the N–N bond length in the optimized structure becomes ≈ 0.06 Å shorter than that in the ground state. This geometry is referred to Q_1. When the symmetry restriction is relaxed to C_2, the N–N bond becomes now longer than that in the ground state and is twisted dramatically. This geometry is denoted Q_2 (fig. 3). The energies of the ground and $T_1(B_1(n\pi^*))$ states calculated at the HF level with the 4-31G basis for this geometry are -262.11798 and -262.14303 au, respectively. This means that the energy of the ground state is higher than that of the T_1 state in this non-planar geometry and that potential crossing between the T_1 and S_0 states occurs (fig. 4).

In order to consider the effect of electron correlation, the energies of the S_0 and T_1 states were calculated by the SAC and SAC CI methods. The energies are -262.33451 and -262.32625 au, respectively, and the wavefunction of the T_1 state is represented by

$$\Psi(T_1) = 0.966(n_- - \pi_1^*) + 0.133(\pi_1 - \pi_1^*),$$

where (a–b) represents the excited configuration with the electron excitation from the a orbital to b orbital. Note that the S_0 state now becomes lower than the T_1 state, and the energy of the T_1 state is higher than that in the planar structure as shown

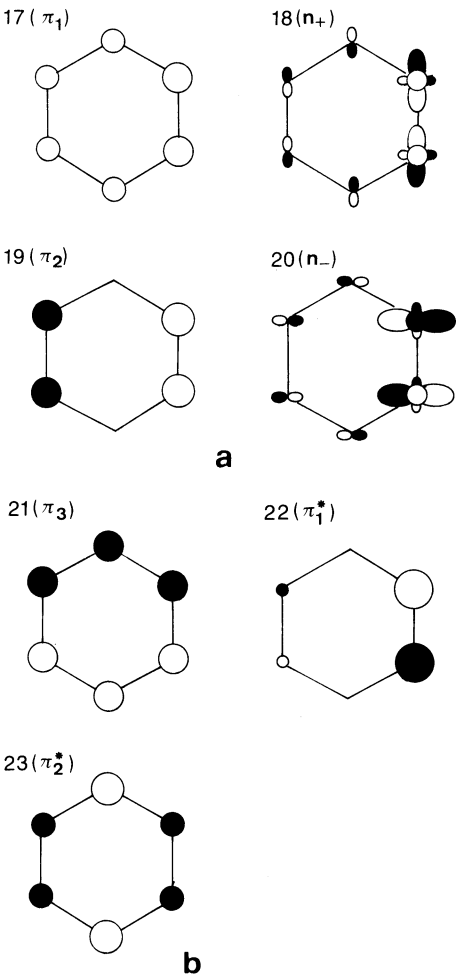

Fig. 2. Schematic representation of MOs which participate in the low-lying excited states. The number is the order of the MOs determined by the 4-31G SCF calculation. For convenience the nomenclature in parentheses is as used in the text.

in fig. 4. This result suggests that the stable geometry of the T_1 state is planar. However, from the wavefunction (T_1), we find that the HF approximation is poor at the twisted geometry because it cannot include the $n\pi^*-\pi\pi^*$ mixing.

In order to see the effect of electron correlation on the N–N bond length, we draw a potential curve along the coordinate to distort the molecule from Q_0 to Q_1 by using the SAC and SAC CI calculation at the STO-3G level. The potential curve shown in fig. 5 indicates that the energies of

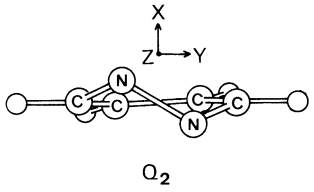

Fig. 3. The optimized geometry of the $^3B_1(n\pi^*)$ state at the HF level of approximation with the restriction of C_2 symmetry (Q_2).

the ground state and the T_1 state are rather insensitive to the N–N bond length. The optimized geometry (Q_3) for T_1 calculated by including electron correlation is only slightly different from Q_1, as shown in fig. 5. In order to check the planarity, we calculate the energies for the non-planar geometry with twisting from Q_3 by using the HF SCF, SAC, and SAC CI techniques. The HF energy for the non-planar geometry is lower than that for the planar geometry, but this order is reversed when

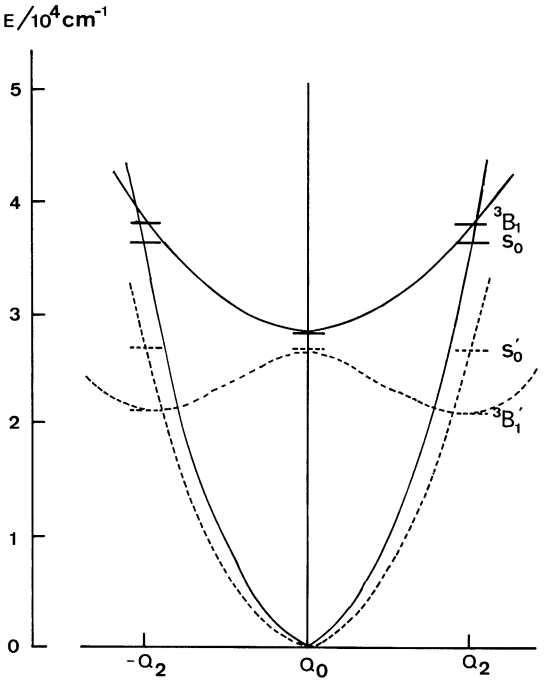

Fig. 4. The potential curve along the distortion coordinate from $Q_0 \rightarrow Q_2$ calculated with the 4-31G basis set at the HF level (dotted curve) and by the SAC and SAC CI methods (solid curve).

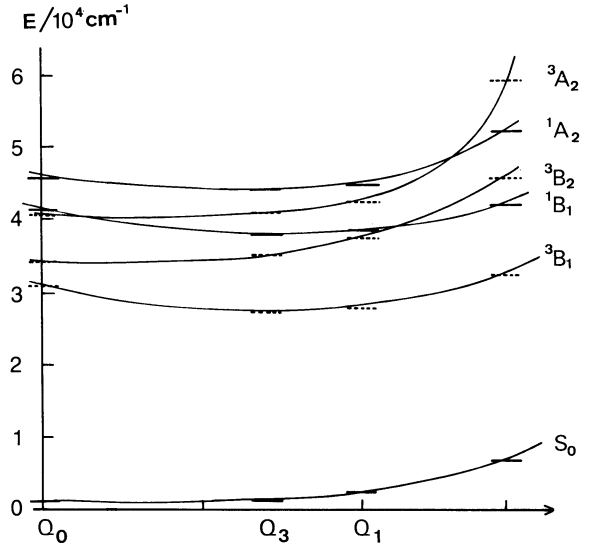

Fig. 5. The potential curve along the distortion coordinate $Q_0 \rightarrow Q_1$ (fig. 1c) calculated with the STO-3G basis set by using the SAC and SAC CI methods.

electron correlation is included in the calculation. Thus we can conclude that the planar geometry is more stable than the non-planar geometry regardless of the N–N bond length.

The above conclusion is consistent with the experimental results. The sublevel decay rate constants of the T_1 state measured by the TREPR method [8] are highly selective ($k_y \gg k_x, k_z$), which is indicative of the planar structure of the T_1 state. The S_0–T_1 absorption spectrum measured by Innes et al. [12] also supported the planarity of the T_1 state.

3.4. The potential surface and the radiationless transition

From fig. 4, we notice that the force constant along the coordinate which distorts the molecule from Q_0 to Q_2 in the $^3B_1$ state (hereafter the mode along this coordinate is called K mode) is much smaller than that in the ground state. The small force constant may be related to the cis–trans isomerization of azo compounds. It is known experimentally that acyclic azo compounds such as diimide isomerize in their lowest excited states [23]. This isomerization can be explained theoretically by the fact that the lowest excited $n\pi^*$ states of such azo compounds are stabilized in the 90° twisted structures [24]. Since the spin density of the $^3B_1(n\pi^*)$ state of pyridazine is localized on the two nitrogen atoms, the character of the $^3B_1$ state must be similar to those of the acyclic azo compounds (table 3). Therefore, the N–N bond tends to be twisted in the T_1 state. However, the delocalized electrons in the other orbitals tend to keep the molecule planar. Combination of these two effects may result in softness of the K mode.

Table 3
Coordinates of the $^3B_1(n\pi^*)$ state with the optimized C_{2v} geometry

	X (Å)	Y (Å)	Z (Å)
N 1	−0.3770	−0.6153	−0.0256
C 3	−0.0106	−0.3778	−1.2346
C 5	0.0530	−0.7416	−2.3849
H 7	0.0095	−2.4560	−1.1298
H 9	0.1732	−1.2657	−3.3334

Reduction of the vibrational frequency of this mode is considered to play an important role in causing a very fast T_1–S_0 decay. The main route of the T_1–S_0 ISC involves the direct spin–orbit coupling with one-center integrals. The radiationless decay rate constant k^{nr} is given by [25]

$$k^{nr} = A\,|\langle n\,|\,H_{so}\,|\,\pi\rangle\,|^2 \rho(E_T)\,F,$$

where A is a constant. $\rho(E_T)$ is the density of the ground vibronic states in the energy region of E_T and F is the Franck–Condon (FC) factor between the S_0 and T_1 states. Since the spin density of the π^* orbital is localized on the two nitrogen atoms, the integral $\langle n\,|\,H_{so}\,|\,\pi^*\rangle$ is large, but it is not sufficient to explain the observed very large k^{nr}. Therefore, the FC factor must be very large to explain the observed large k^{nr}. Theoretically, when the positions of the minima or the curvatures of the potential surfaces of the two states are very different (displaced or distorted oscillators, respectively), the FC factor can be large [26]. In the pyridazine case, however, the potential curve calculated by including electron correlation (fig. 5) shows that the N–N bond lengths as well as the curvatures of the potential curves of the ground and T_1 states along the N–N stretching mode are

very similar. Therefore, the FC factor due to the displaced and distorted oscillators along this mode is not important. It is more likely that the distorted oscillator along the K mode (fig. 4) is responsible for the large FC factor. The FC factor for the distorted oscillator is given by [26]

$$F = (1-\xi^2)^{1/2}\xi^{\nu}\frac{1\times 3\times 5\times\cdots\times(\nu-1)}{2\times 4\times 6\times\cdots\times\nu},$$

$$\xi^2 = \frac{[\omega_k-\omega_k']^2}{[\omega_k+\omega_k']^2}, \quad \nu\text{: even},$$

where ω_k and ω_k' are the frequencies of the K mode in the ground and the excited state, respectively. Then the large difference in the force constant can bring in a very large FC factor.

The importance of the twisted mode localized at the nitrogen atoms in providing a large FC factor is supported by the fact that the other ortho-diazaaromatic compounds such as 3,6-dichloropyridazine, phthalazine and 9,10-diazaphenanthrene all have very short-lived triplet states [27]. The triplet lifetimes of these compounds are of microsecond to submicrosecond order despite the differences in molecular structure.

3.5. On the existence of a nearby S_2 state

In 1978 Innes et al. [12] proposed that the 373 cm^{-1} band in the S_0–S_1 absorption spectrum is the electronic origin of the $S_2(B_1(n\pi^*))$ state. This proposition was also supported by Ueda et al. [13] who studied the SVL fluorescence spectrum of pyridazine. However, existence of the $S_2(B_1(n\pi^*))$ state in the vicinity of the S_1 state is not predicted by the present calculation. In fact, the present calculation predicts the $S_2(A_2(n\pi^*))$ and the second $^1B_1(n\pi^*)$ states to be 6600 and 21000 cm^{-1} above the S_1 origin, respectively. Even if we take errors in the calculated results into consideration, presence of the $S_2(B_1(n\pi^*))$ state in the vicinity of the origin of the S_1 state does not seem likely. Although Rydberg states were not calculated in the present study, the intensity and the low-lying nature (26600 cm^{-1}) of the band exclude the involvement of such states.

Innes et al. have considered the possibility that this band is due to the overtone band K_0^2 of the out-of-plane vibration, but excluded this possibility mainly because the K_2^2 band was not detected in the fluorescence spectrum obtained by excitation at the 373 cm^{-1} band [12]. When the K mode of the excited state is very different from that of the ground state as indicated by the result of the present calculation, the intensity corresponding to the K_2^2 band might be diluted over many modes of the ground state which compose the K mode (K = 16a + 5 + 4 + ···). Such a mode mixing should also lead to a complex S_0–S_1 absorption spectrum as observed. However, at present we are unable to offer an entirely satisfactory explanation for the origin of the 373 cm^{-1} band.

Finally we mention the location of the T_2 state. The temperature dependence of the zero field splittings of the T_1 state measured by the TREPR technique is very small indicating that the T_2 state is not close to the T_1 state [9]. This is consistent with the present result that the S_2 state is not close to the S_1 state.

4. Summary

The geometries and energies of the ground and excited states of pyridazine have been calculated by ab initio calculations including electron correlation. It is concluded that electron correlation plays an essential role in determining the geometries of the excited states of pyridazine. The optimized geometry of the $^3B_1(n\pi^*)$ state is planar, which is consistent with the results of S_0–T_1 absorption and the TREPR measurements. On the basis of the present calculation it is proposed that the main reason for the very fast T_1–S_0 decay is the increased FC factor due to the shallow potential for the out-of-plane distortion of the N–N bond. The calculation also shows that the S_2 state is not likely to be close to the S_1 origin, contrary to the claim based on spectroscopic measurements.

Acknowledgement

We thank the computer center of the Institute for the Molecular Science for the use of the HITAC

M-200 computer and also thank the Data Processing Center of Kyoto University.

References

[1] A.E.W. Knight and C.S. Parmenter, Chem. Phys. 15 (1976) 85.
[2] C.D. Buckley and K.A. McLauchlan, Mol. Phys. 54 (1985) 1.
[3] M.A. El-Sayed, J. Chem. Phys. 36 (1962) 573.
[4] R.M. Hochstrasser and C. Marzzacco, J. Chem. Phys. 46 (1967) 4155.
[5] K. Yamamoto, T. Takemura and H. Baba, Bull. Chem. Soc. Japan 48 (1975) 2599.
[6] J. Leclercq, D. Yvan and J.M. Leclercq, Chem. Phys. 22 (1977) 233.
[7] C.A. Masmanidis, H.H. Jaffe and R.L. Ellis, J. Phys. Chem. 79 (1975) 2052.
[8] B.J. Cohen and L. Goodman, J. Chem. Phys. 46 (1967) 713.
[9] M. Terazima, S. Yamauchi and N. Hirota, Chem. Phys. Letters 120 (1985) 321; J. Chem. Phys. 84 (1986) 3679.
[10] G.D. Neykov, J. Mol. Struct. 114 (1984) 407.
[11] J.E. Ridley and M.C. Zerner, Theoret. Chim. Acta 42 (1976) 223.
[12] K.K. Innes, W.C. Tincker and E.F. Pearson, J. Mol. Spectry. 36 (1970) 114;
B.D. Ranson and K.K. Innes, J. Mol. Spectry. 69 (1978) 394.
[13] E. Ueda, Y. Udagawa and M. Ito, Chem. Letters (1981) 873.
[14] J. Ridley and M. Zerner, Theoret. Chim. Acta 32 (1973) 111;
S.-Y. Chen and R.M. Hedges, Theoret. Chim. Acta. 31 (1973) 275.
[15] H. Nakatsuji, Chem. Phys. Letters 59 (1978) 362; 67 (1979) 329;
[16] H. Nakatsuji, Chem. Phys. 75 (1983) 425;
H. Nakatsuji and K. Hirao, J. Chem. Phys. 68 (1978) 2053.
[17] H. Nakatsuji, J. Chem. Phys. 80 (1984) 3703, and references therein.
[18] H. Nakatsuji, K. Ohta and K. Hirao, J. Chem. Phys. 75 (1981) 2952.
[19] H. Nakatsuji, Intern. J. Quantum Chem. Symp. 17 (1983) 241.
[20] H. Nakatsuji, O. Kitao and T. Yonezawa, J. Chem. Phys. 83 (1985) 723.
[21] A. Almenningen, G. Bjørnsen, T. Ottersen, R. Seip and T.G. Strand, Acta Chem. Scand. A31 (1977) 63.
[22] B.R. Brooks, P. Saxe, W.D. Ladig and M. Dupius, Program Library GAMESS (No. 481) of the Computer Center of the Institute for Molecular Science (1981).
[23] N.J. Turro, Modern molecular photochemistry (Benjamin/Cummings, Manlo Park, 1978).
[24] Y. Osamura, K. Kitaura, K. Nishimoto and S. Yamabe, Chem. Phys. Letters 63 (1979) 406.
[25] R.M. Hochstrasser, Chem. Phys. Letters 15 (1972) 316.
[26] W. Siebrand, J. Chem. Phys. 46 (1967) 440;
E. Hutchisson, Phys. Rev. 36 (1930) 410;
C. Manneback, Physica 17 (1951) 1001.
[27] M. Terazima, S. Yamauchi and N. Hirota, unpublished results.